ROSE 2008 – IEEE International Workshop
on Robotic and Sensors Environments
Ottawa – Canada, 17-18 October 2008

Dynamic Modeling of a Rotating Beam Having a Tip Mass

Shengjian Bai[1], Pinhas Ben-Tzvi [2], Qingkun Zhou[1,3], Xinsheng Huang[1]
[1] College of Mechatronics Engineering and Automation, National University of Defense Technology, Changsha Hunan 410073, P. R. China
[2] Department of Mechanical and Aerospace Engineering, School of Engineering and Applied Science, The George Washington University, 801 22nd St., NW, Washington, DC 20052
[3] Department of Mechanical and Industrial Eng., University of Toronto, 5 King's College Rd., Toronto, ON, Canada M5S 3G8

Abstract– *This paper presents a dynamic model of a flexible hub-beam system with a tip mass. With the consideration of the second-order term of the coupling deformation field, dynamic equations of the flexible hub-beam system are developed by using assumed mode method (AMM) and Lagrangian principle. The corresponding dynamics model of the tip mass is developed in a consistent manner. Numerical simulations and Theoretical analysis show that the second-order term has a significant effect on the dynamic characteristics of the system and the dynamic stiffening is accounted for. The effect of tip mass on dynamic behavior of the multibody system is also discussed.*

Keywords – *dynamic stiffening, assumed mode method, flexible beam.*

I. INTRODUCTION

Rotating flexible beams are used to model light robot arms, elastic linkage, helicopter rotors, satellite solar array, and like systems. Modeling and control of systems involving interconnected rigid structures and flexible appendages is a difficult task to accomplish, as most of these systems generally involve complex dynamics characterized by nonlinearities and strong coupling between flexible and rigid modes. Moreover, modern engineering technology is leading to ever more demanding performance criteria, such as high rotating speed and large angular maneuvering, increasing precision and pointing accuracy. These criteria have posed serious difficulties for all currently advocated control design methodologies. Proper dynamic modeling of the system is a foundation for further research, such as analysis of the dynamic characteristics and various controller designs.

The hybrid coordinate approach is currently the most widely used method, which describes the deformation field of flexible and rigid bodies separately. The mechanical systems undergoing high–speed can produce the phenomenon of dynamic stiffening [1,2] due to the coupling between rigid motion and elastic deflection, and traditional dynamic analysis can hardly deal with it. The deformation field, commonly used in structural dynamics, is adopted in order to calculate the kinematics of flexible components in the system. Therefore, modal characteristic changes due to high rotational speeds are not included in the traditional dynamic equations [3].

In most cases, problems arise not because of a lack of available analytical/numerical design procedures but because of our failure to recognize and appreciate the mechanism of dynamic stiffening. Unlike the research reported in [4,5] where the attempt was to "capture" the dynamic stiffening terms, Hong et al [6-8] studied the mechanism of dynamic stiffening, and concluded that the coupling deformation field can explain the phenomenon. Researches [7–9] indicated that the coupling term not included in traditional linear deformation field can have significant effect on the dynamic characteristics of the multibody system when it undergoes large rigid–body motion. The paper [7] investigated a hub–beam system by using finite element method, and pointed out that traditional hybrid coordinate approach may lead to erroneous result in some high–speed systems. In Ref. [9], Kane's methods and AMM were employed to investigate rigid-flexible dynamics of spacecraft with solar panels. In this paper, the first–order approximated model (FOAM) of a hub–beam system is obtained by using the AMM and Lagrangian principle. The corresponding dynamic model of the tip mass is developed in a consistent manner.

This paper is organized as follows. Section II describes the flexible hub–beam system and defines the symbols used. In section III, dynamic equations of the flexible system are developed. In section IV, numerical simulations and comparisons with traditional linear approximated model (TLAM) are presented to demonstrate the validity of the developed model (FOAM). Furthermore, the effect of tip mass on dynamics behavior of the hub–beam system is also discussed in the section. The paper concludes with a discussion provided in section V.

II. SYSTEM DESCRIPTION

The system to be analyzed as shown in Fig. 1 consists of a cantilever beam *B* built into a rigid body *H*.

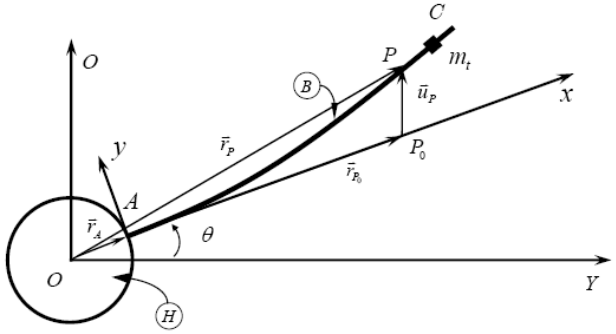

Fig. 1 Beam attached to moving rigid hub

978-1-4244-2595-2/08/$25.00 ©2008 IEEE

The coordinates XY and xy in the figure are defined as the inertial frame and the reference frame, respectively. $\vec{u}_p$ is denoted as the flexible deformation vector at point P with respect to the xy frame, and $\vec{r}_A$ is the radius vector of point A on the hub. θ is considered as rigid body coordinate. After deformation, the point P_0 moves to point P.

The beam is characterized by a natural length L, material properties E, ρ, and cross-sectional properties A, I, defined as follows. E and ρ are the modulus of elasticity, and the mass per unit volume of the beam, respectively. The area of the cross section is denoted as A, and the beam area moment of inertia is denoted as I.

III. EQUATIONS OF MOTION

As shown in Fig.1, the position vector from O to P in the XY frame can be expressed as:

$$\vec{r}_p = \vec{r}_A + \vec{r}_0 + \vec{u}_p \tag{1}$$

where $\vec{r}_A = \overrightarrow{OA}$, $\vec{r}_0 = \overrightarrow{AP}_0$, and $\vec{u}_p = \overrightarrow{P_0P}$. The coordinates of $\vec{r}_A$ and $\vec{r}_0$ in the OXY frame are represented by $\boldsymbol{r}_A$ and $\boldsymbol{r}_0$, respectively.

As shown in Fig.2, The coordinate of the deformation vector $\vec{u}_p$ can be represented as:

$$\boldsymbol{u}_p = (u \quad v)^T = (w_1 + w_c \quad w_2)^T \tag{2}$$

where u and v are the deformation quantities of the point P_0 in x direction and y direction in the xy frame, respectively; w_1 represents the pure axial deformation, w_2 represents the transverse deformation along the y–axis. w_c is the deformation associated with the foreshortening quantity due to w_2, represented as [7,8]:

$$w_c = -\frac{1}{2}\int_0^x \left(\frac{\partial w_2}{\partial x}\right)^2 \mathrm{d}x \tag{3}$$

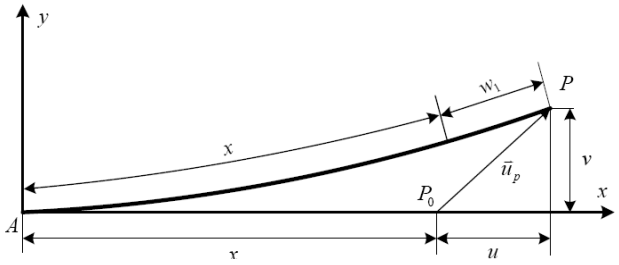

Fig.2 Beam description of deformation

The coordinate of $\vec{r}_p$ (1) in the XY frame may be written as

$$\boldsymbol{r}_p = \boldsymbol{r}_A + \boldsymbol{\Theta}(\boldsymbol{r}_0 + \boldsymbol{u}_p) = \boldsymbol{\Theta}(r_A\mathbf{e} + \boldsymbol{r}_0 + \boldsymbol{u}_p) \tag{4}$$

where $\boldsymbol{r}_0 = (x \quad 0)^T$, $\boldsymbol{u}_p = (u \quad v)^T$, $\boldsymbol{e} = (1 \quad 0)^T$, and $\boldsymbol{r}_A = r_A(\cos\theta \quad \sin\theta)^T$, as shown in Fig.2, the variable x is the coordinate of the point P_0 in the xy frame, the parameter $\boldsymbol{\Theta}$ is a direction cosine matrix which is the xy frame with respect to the XY frame, given by:

$$\boldsymbol{\Theta} = \begin{pmatrix} \cos\theta & -\sin\theta \\ \sin\theta & \cos\theta \end{pmatrix} \tag{5}$$

where θ is the angular displacement of the hub.

The first-order derivative of $\boldsymbol{r}_P$ may be expressed as

$$\dot{\boldsymbol{r}}_P = \dot{\boldsymbol{\Theta}}\mathbf{I}(r_A\mathbf{e} + \boldsymbol{r}_0 + \boldsymbol{u}_p) + \boldsymbol{\Theta}\dot{\boldsymbol{u}}_p \tag{6}$$

where

$$\mathbf{I} = \begin{pmatrix} 0 & -1 \\ 1 & 0 \end{pmatrix}, \qquad \dot{\boldsymbol{u}}_p = \begin{pmatrix} \dot{w}_1 - \dot{w}_c \\ \dot{w}_2 \end{pmatrix} \tag{7}$$

From Eq.(6), we can derive

$$\begin{aligned} \dot{\boldsymbol{r}}_P^T\dot{\boldsymbol{r}}_P = \dot{\theta}^2\left\{(r_A + w_1 + w_c + x)^2 + w_2^2\right\} + (\dot{w}_1 + \dot{w}_c)^2 + \dot{w}_2^2 \\ + 2\dot{\theta}\left\{(r_A + w_1 + w_c + x)\dot{w}_2 - (\dot{w}_1 + \dot{w}_c)v\right\} \end{aligned} \tag{8}$$

The kinetic energy of the hub–beam system is written as

$$T = T_h + T_b + T_t = \frac{1}{2}J_h\dot{\theta}^2 + \frac{1}{2}\int_0^L \dot{\boldsymbol{r}}_P^T\dot{\boldsymbol{r}}_P dx + \frac{1}{2}\boldsymbol{m}_t\dot{\boldsymbol{r}}_t^T\dot{\boldsymbol{r}}_t \tag{9}$$

where T_h, T_b and T_t are the kinetic energy of the hub, of the beam and of the tip mass, respectively. J_h is the rotational inertia of the hub. m_t is the weight of the tip mass. r_t is the coordinate of the position vector from A to the tip mass.

By using Euler–Bernoulli theory, the potential energy is given by

$$U = \frac{1}{2}\int_0^L EA\left(\frac{\partial w_1}{\partial x}\right)^2 dx + \frac{1}{2}\int_0^L EI\left(\frac{\partial^2 w_2}{\partial x^2}\right)^2 dx \tag{10}$$

in which E is Young's modulus, A is the cross–sectional area and I is the area moment of inertia.

The AMM is used to discretize the elastic beam, then the deformation u and v can be represented as

$$u(x,t) = \sum_{i=1}^{n}\phi_i^{(1)}(x)q_i^{(1)}(t), \quad v(x,t) = \sum_{i=1}^{n}\phi_i^{(2)}(x)q_i^{(2)}(t) \tag{11}$$

where $\phi_i^{(1)}(x)$ and $\phi_i^{(2)}(x)$ are the admissible functions, $q_i^{(1)}(t)$ and $q_i^{(2)}(t)$ are the mode generalized coordinates, and n refers to the number of included modes. In subsequent derivations, $\boldsymbol{\phi}_1(x)$, $\boldsymbol{\phi}_2(x)$, $\boldsymbol{q}_1(t)$ and $\boldsymbol{q}_2(t)$ are adopted to represent the vectors of $\phi_i^{(1)}(x)$, $\phi_i^{(2)}(x)$, $q_i^{(1)}(t)$ and $q_i^{(2)}(t)$, respectively.

3.1 Equations of motion at the element level

To produce equations of motion in a compact form, the following element coefficients and matrices are introduced

$$J_b = \int_0^L \rho A(r_A + x)^2 dx \tag{12}$$

$$\boldsymbol{K}_1 = \int_0^L EA\left(\frac{\partial \phi_1(x)}{\partial x}\right)^T \frac{\partial \phi_1(x)}{\partial x} dx \tag{13}$$

$$\boldsymbol{K}_2 = \int_0^L EI\left(\frac{\partial^2 \phi_2(x)}{\partial x^2}\right)^T \frac{\partial^2 \phi_2(x)}{\partial x^2} dx \tag{14}$$

$$\boldsymbol{M}_i = \int_0^L \rho A \phi_i^T \phi_i dx, \qquad i = 1,2 \tag{15}$$

$$\boldsymbol{V}_i = \int_0^L \rho A (r_A + x)\phi_i dx \qquad i = 1,2 \tag{16}$$

$$\boldsymbol{D} = \int_0^L \rho A (r_A + x)\boldsymbol{S}(x) dx \tag{17}$$

$$\boldsymbol{R} = \int_0^L \rho A \phi_1^T \phi_2 dx \tag{18}$$

where J_b is the rotational inertia of the beam about the hub center, the matrices $\boldsymbol{K}_1 \in R^{n\times n}$ and $\boldsymbol{K}_2 \in R^{n\times n}$ are the conventional stiffness matrices, $\boldsymbol{M}_i \in R^{n\times n}$, $i = 1,2$ are generalized elastic mass matrix, the matrix $\boldsymbol{D}$ results from the second order term of the coupling deformation field (3), the matrix $\boldsymbol{R}$ results from the gyroscopic effects, $\boldsymbol{S}(x)$ results from w_c and is represented as:

$$\boldsymbol{S}(x) = \int_0^x \frac{\partial \phi_2^T(\xi)}{\partial \xi}\frac{\partial \phi_2(\xi)}{\partial \xi} \mathrm{d}\xi \tag{19}$$

It is important to note that, the matrix $\boldsymbol{D}$ is *non-negative definite* because $\boldsymbol{S}(x)$ is a non-negative definite matrix.

Using AMM with n assumed modes, Eqs.(9) and (10) can be rewritten as:

$$\begin{aligned} T = \dot{\theta}^2 \Big(& \frac{1}{2}J_h + \frac{1}{2}J_b + \boldsymbol{V}_1\boldsymbol{q}_1 + \frac{1}{2}\boldsymbol{q}_1^T\boldsymbol{M}_1\boldsymbol{q}_1 + \frac{1}{2}\boldsymbol{q}_2^T\boldsymbol{M}_2\boldsymbol{q}_2 \\ & - \frac{1}{2}\boldsymbol{q}_2^T\boldsymbol{D}\boldsymbol{q}_2 \Big) + \dot{\theta}\left(\boldsymbol{V}_2\dot{\boldsymbol{q}}_2 + \boldsymbol{q}_1^T\boldsymbol{R}\dot{\boldsymbol{q}}_2 - \boldsymbol{q}_2^T\boldsymbol{R}^T\dot{\boldsymbol{q}}_1\right) \\ & + \frac{1}{2}\dot{\boldsymbol{q}}_1^T\boldsymbol{M}_1\dot{\boldsymbol{q}}_1 + \frac{1}{2}\dot{\boldsymbol{q}}_2^T\boldsymbol{M}_2\dot{\boldsymbol{q}}_2 \end{aligned} \tag{20}$$

$$U = \frac{1}{2}\boldsymbol{q}_1^T\boldsymbol{K}_1\boldsymbol{q}_1 + \frac{1}{2}\boldsymbol{q}_2^T\boldsymbol{K}_2\boldsymbol{q}_2 \tag{21}$$

The governing equations of motion can now be obtained through application of the Lagrangian principle

$$\frac{d}{dt}\left(\frac{\partial T}{\partial \dot{\eta}_i}\right) - \frac{\partial T}{\partial \eta_i} + \frac{\partial U}{\partial \eta_i} = Q_i \qquad i = 1,2,\cdots,n+1 \tag{22}$$

where η_i are the system generalized coordinates, and Q_i the nonconservative generalized forces due to environmental effects and actuators.

By Substituting Eqs.(20) and (21) into Eq.(22), the equations of motion of the flexible system at element level in compact form can be derived as:

$$\begin{aligned} & \begin{bmatrix} M_{\theta\theta} & \boldsymbol{M}_{\theta q_1} & \boldsymbol{M}_{\theta q_2} \\ \boldsymbol{M}_{q_1\theta} & \boldsymbol{M}_{q_1 q_1} & \boldsymbol{0} \\ \boldsymbol{M}_{q_2\theta} & \boldsymbol{0} & \boldsymbol{M}_{q_2 q_2} \end{bmatrix}\begin{bmatrix} \ddot{\theta} \\ \ddot{\boldsymbol{q}}_1 \\ \ddot{\boldsymbol{q}}_2 \end{bmatrix} + 2\dot{\theta}\begin{bmatrix} 0 & \boldsymbol{0} & \boldsymbol{0} \\ 0 & \boldsymbol{0} & \boldsymbol{G}_{q_1 q_2} \\ 0 & \boldsymbol{G}_{q_2 q_1} & \boldsymbol{0} \end{bmatrix}\begin{bmatrix} \dot{\theta} \\ \dot{\boldsymbol{q}}_1 \\ \dot{\boldsymbol{q}}_2 \end{bmatrix} \\ & + \begin{bmatrix} 0 & \boldsymbol{0} & \boldsymbol{0} \\ 0 & \boldsymbol{K}_{q_1 q_1} & \boldsymbol{0} \\ 0 & \boldsymbol{0} & \boldsymbol{K}_{q_2 q_2} \end{bmatrix}\begin{bmatrix} \theta \\ \boldsymbol{q}_1 \\ \boldsymbol{q}_2 \end{bmatrix} = \begin{bmatrix} Q_\theta \\ \boldsymbol{Q}_{q_1} \\ \boldsymbol{0} \end{bmatrix} + \begin{bmatrix} \tau \\ \boldsymbol{0} \\ \boldsymbol{0} \end{bmatrix} \end{aligned} \tag{23}$$

where $\boldsymbol{M}_{\theta\theta} \in R^1$ is the rotary inertia of the system, $\boldsymbol{M}_{q_1 q_1} \in R^{n\times n}$ and $\boldsymbol{M}_{q_2 q_2} \in R^{n\times n}$ are the beam generalized elastic mass matrices, $\boldsymbol{M}_{\theta q_1} \in R^{1\times n}$, $\boldsymbol{M}_{\theta q_2} \in R^{1\times n}$, $\boldsymbol{M}_{q_1\theta} \in R^{n\times 1}$ and $\boldsymbol{M}_{q_2\theta} \in R^{n\times 1}$ represent the nonlinear inertia coupling between the motion of the reference frame and the elastic deformations, $\boldsymbol{K}_{q_1 q_1} \in R^{n\times n}$ and $\boldsymbol{K}_{q_2 q_2} \in R^{n\times n}$ are generalized elastic stiffness matrices that are shown to be affected by both the motion of the reference frame and the elastic deformations, Q_θ represents inertia forces, τ is the rotational external torque. The parameters in Eq.(23) are given as follows:

$$\begin{aligned} M_{\theta\theta} = {} & J_h + J_b + \boldsymbol{q}_1^T\boldsymbol{M}_1\boldsymbol{q}_1 + \boldsymbol{q}_2^T\boldsymbol{M}_2\boldsymbol{q}_2 \\ & + 2\boldsymbol{V}_{11}\boldsymbol{q}_1 - \underline{\boldsymbol{q}_2^T\boldsymbol{D}\boldsymbol{q}_2} \end{aligned} \tag{24}$$

$$\boldsymbol{M}_{q_1\theta} = \boldsymbol{M}_{\theta q_1}^T = -\boldsymbol{R}\boldsymbol{q}_2 \tag{25}$$

$$\boldsymbol{M}_{\theta q_2} = \boldsymbol{M}_{q_2\theta}^T = \boldsymbol{V}_{12} + \boldsymbol{q}_1^T\boldsymbol{R} \tag{26}$$

$$\boldsymbol{M}_{q_i q_i} = \boldsymbol{M}_i \qquad i = 1,2 \tag{27}$$

$$\boldsymbol{G}_{q_1 q_2} = -\boldsymbol{G}_{q_2 q_1}^T = -\boldsymbol{R} \tag{28}$$

$$\boldsymbol{K}_{q_1 q_1} = \boldsymbol{K}_1 - \dot{\theta}^2\boldsymbol{M}_1 \tag{29}$$

$$\boldsymbol{K}_{q_2 q_2} = \boldsymbol{K}_2 - \dot{\theta}^2\boldsymbol{M}_2 + \underline{\dot{\theta}^2\boldsymbol{D}} \tag{30}$$

$$Q_\theta = -2\dot{\theta}\left[\left(\boldsymbol{q}_1^T\boldsymbol{M}_1\dot{\boldsymbol{q}}_1 + \boldsymbol{q}_2^T\boldsymbol{M}_2\dot{\boldsymbol{q}}_2\right) + \boldsymbol{V}_1\dot{\boldsymbol{q}}_1 - \underline{\boldsymbol{q}_2^T\boldsymbol{D}\dot{\boldsymbol{q}}_2}\right] \tag{31}$$

$$\boldsymbol{Q}_{q_1} = \dot{\theta}^2\boldsymbol{V}_1^T \tag{32}$$

In Eq.(23), the nonlinear coupling between the rigid–body motion and the elastic deformations can be easily seen. The underlined terms in Eqs.(24), (30) and (31) result from the coupling deformation field. The newly established Eqs.(23)-(32) are called the first-order approximate model (FOAM), and the equations without the underlined terms are called traditional linear approximate model (TLAM).

3.2 Tip mass dynamics

The tip mass, as shown in Fig.1, is located at a distance r_t along the undeformed beam from the point A. It is considered to have a mass m_t. The position vector of the tip mass with respect to the inertial frame XY can be represented as

$$\boldsymbol{r}_m = \boldsymbol{r}_A + \boldsymbol{\Theta}(\boldsymbol{r}_t + \boldsymbol{u}_t) \tag{33}$$

where $\boldsymbol{r}_t = (r_t \quad 0)^T$ is the position vector of the tip mass in the reference frame xy in the undeformed configuration, $\boldsymbol{u}_t$ is the elastic displacement vector of the point on the beam to which the tip mass is attached.

The contribution of the tip mass to the dynamics of the multibody system can also be included by applying the Lagrangian principle. The equations can be represented by the following matrix form

$$\begin{bmatrix} M^l_{\theta\theta} & \boldsymbol{M}^l_{\theta q_1} & \boldsymbol{M}^l_{\theta q_2} \\ \boldsymbol{M}^l_{q_1\theta} & \boldsymbol{M}^l_{q_1 q_1} & \boldsymbol{0} \\ \boldsymbol{M}^l_{q_2\theta} & \boldsymbol{0} & \boldsymbol{M}^l_{q_2 q_2} \end{bmatrix} \begin{bmatrix} \ddot{\theta} \\ \ddot{\boldsymbol{q}}_1 \\ \ddot{\boldsymbol{q}}_2 \end{bmatrix} + 2\dot{\theta} \begin{bmatrix} 0 & \boldsymbol{0} & \boldsymbol{0} \\ \boldsymbol{0} & \boldsymbol{0} & \boldsymbol{G}^l_{q_1 q_2} \\ \boldsymbol{0} & \boldsymbol{G}^l_{q_2 q_1} & \boldsymbol{0} \end{bmatrix} \begin{bmatrix} \dot{\theta} \\ \dot{\boldsymbol{q}}_1 \\ \dot{\boldsymbol{q}}_2 \end{bmatrix} + \begin{bmatrix} 0 & \boldsymbol{0} & \boldsymbol{0} \\ \boldsymbol{0} & \boldsymbol{K}^l_{q_1 q_1} & \boldsymbol{0} \\ \boldsymbol{0} & \boldsymbol{0} & \boldsymbol{K}^l_{q_2 q_2} \end{bmatrix} \begin{bmatrix} \theta \\ \boldsymbol{q}_1 \\ \boldsymbol{q}_2 \end{bmatrix} = \begin{bmatrix} Q^l_\theta \\ \boldsymbol{Q}^l_{q_1} \\ \boldsymbol{0} \end{bmatrix} \tag{34}$$

where the coefficients and matrices are shown in the appendix.

3.3 Equations of motion of the whole system

The equations of motion of the whole system can be obtained from Eqs.(23) and (34) directly by adding the corresponding entries of the generalized matrices. Two different models are developed in order to examine the effect of the second order term. The established equations with and without the underlined terms are called FOAM and TLAM, respectively.

IV. SIMULATIONS AND RESULTS

The physical parameters of the flexible hub-beam system are shown in Table 1. The payload is represented by a point mass m_t at the free end of the beam. The number of included modes n is 5.

Table 1 Physical parameters

Property	Symbol	Value
Beam length	L	8m
Mass per unit volume	ρ	2.7667×10^3 kg/m^3
Cross-Section	A	7.2968×10^{-5}m^2
Young's modulus	E	6.8952×10^{10} N/m^2
Beam area moment of inertia	I	8.2189×10^{-9}m^4
Hub moment of inertia	J_h	200kgm^2
Hub radius	r	0.5m
Tip mass	m_t	0.1kg

The response of the flexible motion is simulated by assuming that the slewing motion follows a prescribed trajectory, and the maneuver profile [2] is given by

$$\dot{\theta} = \begin{cases} \dfrac{w_f}{t_f} - \dfrac{w_f}{2\pi}\sin\left(\dfrac{2\pi}{t_f}t\right), & 0 \le t \le t_f \\ w_f, & t > t_f \end{cases} \tag{35}$$

where w_f and t_f represent the velocity of the hub at the end of the maneuver, and the time to reach the maximum velocity, respectively.

4.1 Vibration response of hub-beam system

Consider first FOAM of the hub–beam system without tip mass. For $w_f = 5rad/s$, and $t_f = 30s$, the resulting response of the first five modes of the flexible hub–beam system is shown in Fig. 3.

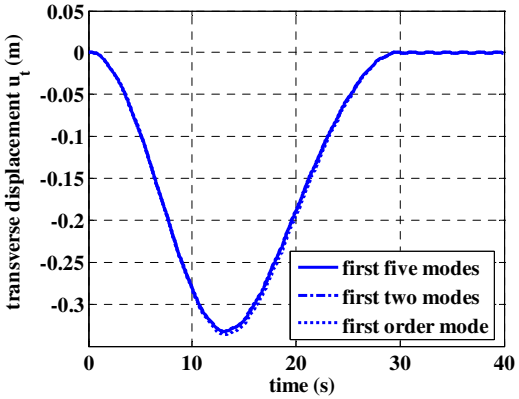

(a) Response of transverse displacement

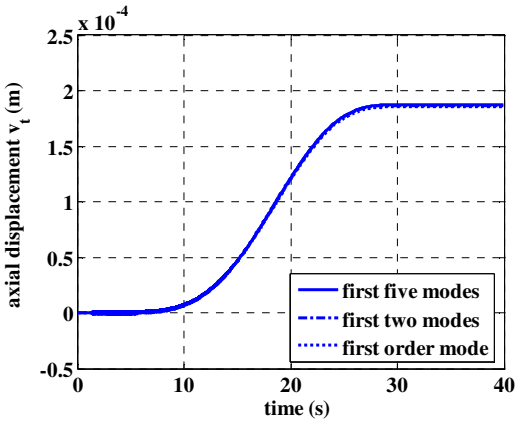

(b) Response of axial displacement

Fig.3 Response of beam vibration to prescribed slew maneuver

It can be seen that the peak response of the transverse displacement is approximately 1500 times larger than that of the axial displacement. As shown in Fig. 2 (a), the response of the first two modes dominates over the response of the higher modes. Thus, a simplified equation of motion of hub-

beam system can be obtained from Eq.(23) by deleting the elements related to $\boldsymbol{q}_1$ and $\dot{\boldsymbol{q}}_1$:

$$\begin{bmatrix} M_{\theta\theta} & \boldsymbol{M}_{\theta q_2} \\ \boldsymbol{M}_{q_2\theta} & \boldsymbol{M}_{q_2q_2} \end{bmatrix}\begin{bmatrix} \ddot{\theta} \\ \ddot{\boldsymbol{q}}_2 \end{bmatrix}+\begin{bmatrix} 0 & \boldsymbol{0} \\ \boldsymbol{0} & \boldsymbol{K}_{q_2q_2} \end{bmatrix}\begin{bmatrix} \theta \\ \boldsymbol{q}_2 \end{bmatrix}=\begin{bmatrix} Q_\theta \\ \boldsymbol{0} \end{bmatrix}+\begin{bmatrix} \tau \\ \boldsymbol{0} \end{bmatrix} \quad (36)$$

where $M_{\theta\theta}$, $\boldsymbol{M}_{\theta q_2}$, $\boldsymbol{M}_{q_2\theta}$, $\boldsymbol{M}_{q_2q_2}$, $\boldsymbol{K}_{q_2q_2}$ and Q_θ can also be obtained by deleting the elements related to $\boldsymbol{q}_1$ and $\dot{\boldsymbol{q}}_1$ in (24) , (26), (27), (30) and (31). It is noted that the simplified model can be used for controller design.

Fig. 4 shows the resulting simulations of TLAM, and FOAM for comparison. The vibrational responses of the flexible beam diverge when the angular velocity is larger than 3rad/s. It should be noted that the resulting tip displacement of TLAM has exceed the assumption of small deformation. When the angular velocity is smaller than 3rad/s but close to the critical value, e.g., 2.8rad/s, the maximum tip deflection of TLAM is much larger than that of FOAM, which are approximately 0.49m and 0.22m, respectively. Moreover, the residual vibration amplitude of TLAM is approximately 100 times larger than that of FOAM. It can be concluded that TLAM is invalid in describing the deformation of multibody system in high–speed cases.

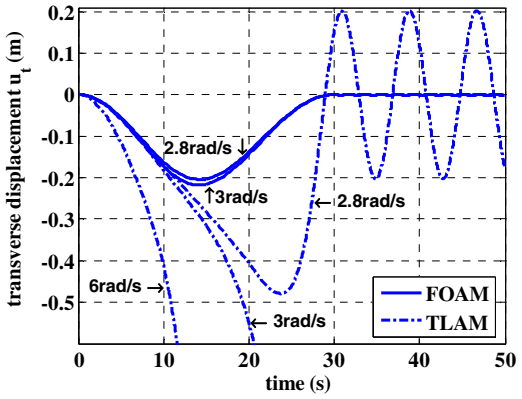

(a) Transverse response of the tip of the beam

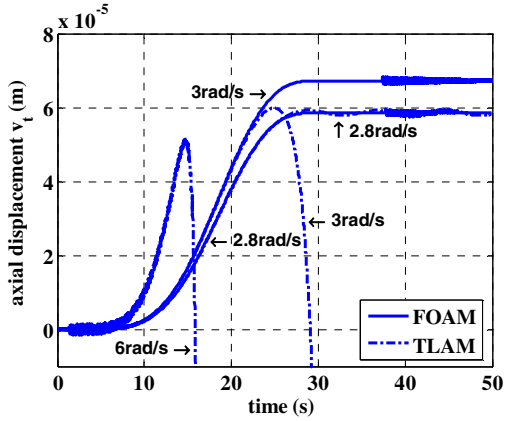

(b) Axial response of the tip of the beam

Fig.4 Response of beam vibration with respect to different angular velocities

Because the second order term in deformation is not included, the generalized elastic stiffness matrix in the TLAM is expressed as $\boldsymbol{K}_{q_2q_2}=\boldsymbol{K}_2-\dot{\theta}^2\boldsymbol{M}_2$. From this expression, it is seen that the stiffness matrix may be negative definite when the angular velocity surpasses a critical value. In fact, it can be calculated from Eq.(30) that the critical angular velocity is 2.91rad/s. This is the first order natural circle frequency of the beam according to Table 2. The frequencies evaluated with TLAM are 'softening' compared to the natural frequencies. On the other hand, the generalized elastic stiffness matrix in FOAM is expressed as $\boldsymbol{K}_{q_2q_2}=\boldsymbol{K}_2-\dot{\theta}^2\boldsymbol{M}_2+\underline{\dot{\theta}^2\boldsymbol{D}}$, in which the underlined term $\dot{\theta}^2\boldsymbol{D}$ is non–negative definite, and can make $\boldsymbol{K}_{q_2q_2}$ definite positive.

Table 2 The first five vibration frequencies (Hz)

Mode oder	1	2	3	4	5
Natural frequency	0.4635	2.9047	8.1332	15.9377	26.3462
TLAM (1 rad/s)	0.4353	2.9003	8.1316	15.9369	26.3457
FOAM (1 rad/s)	0.4714	2.9308	8.1618	15.9682	26.3776

As shown in Table 2, the natural vibration frequency is larger than that evaluated with TLAM, but less than that evaluated with FOAM. i.e., the second order term in coupling deformation field has a 'stiffening' effect on the frequencies of the multibody system in high-speed case. The difference values become larger when the speed increases.

4.2 Vibration response of hub-beam system with tip mass

The general elastic stiffness matrix of the whole system in TLAM is $\boldsymbol{K}_{22}=\boldsymbol{K}_2-\dot{\theta}^2\boldsymbol{M}_2-m_t\phi_2^T(l)\phi_2(l)\dot{\theta}^2$, which shows that the positive definite property of the stiffness matrix in TLAM is determined by the position r_t , the angular velocity $\dot{\theta}$ and the mass m_t . It is known that the positive definite property of $\boldsymbol{K}_{22}$ is determined by the sign of its eigenvalues. Fig. 5 shows this relationship.

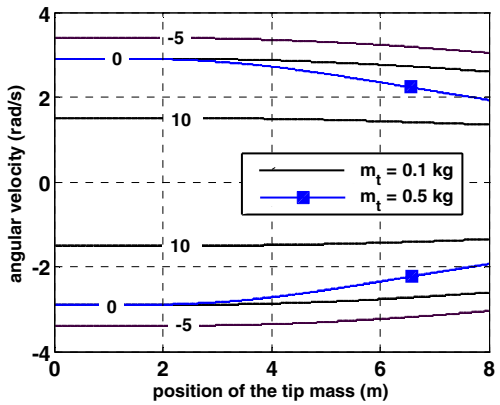

Fig. 5 The dominate eigenvalues of $\boldsymbol{K}_{22}$

As shown in the figure, the critical velocity is 2.91rad/s when m_t is located on the hub ($l = 0$). If the angular velocity surpasses the critical value, the dominate eigenvalues of $\boldsymbol{K}_{22}$ will be negative , which can explain the simulation results (3rad/s) in Fig. 4. When the tip mass is located at the tip of the beam, the critical velocities are 2.60rad/s and 1.91rad/s for the cases m_t=0.1kg and m_t=0.5kg, respectively. Fig. 6 shows the transverse displacement of TLAM for the above two cases. For the case m_t=0.5kg, TLAM is failed to describe the deformation of the flexible beam when the angular velocity is 2.0rad/s. However for the same angular velocity, the simulation result of TLAM is almost the same as that of FOAM when m_t=0. It is seen that, the tip mass will decrease the critical angular velocity; moreover, the higher the weight, the lower the critical value.

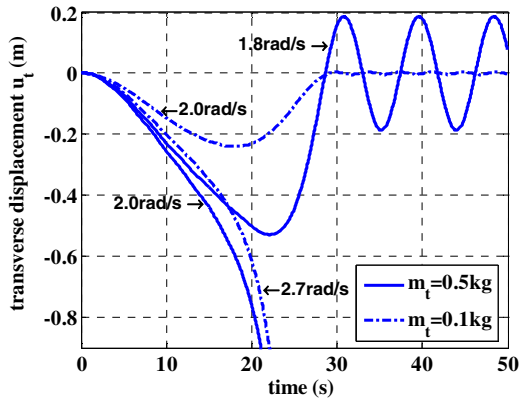

Fig.6 Response of TLAM system with tip mass

The generalized elastic stiffness matrix of the tip mass is expressed as $\boldsymbol{K}^l_{q_2q_2} = -m_t\phi_2^T(l)\phi_2(l)\dot{\theta}^2$, which has a 'softening' effect on the flexible hub–beam system. Because the second order term in coupling deformation is included, the generalized elastic stiffness matrix in FOAM has a term $m_t\left(r_A + L\right)\dot{\theta}^2\boldsymbol{S}$, which acts as 'stiffening' effect.

V. CONCLUSIONS

In this paper, the FOAM of a flexible hub–beam system with a tip mass has been presented by using AMM and Lagrangian principle. The second order term in the coupling deformation field has a 'stiffening' effect on the frequencies and the dynamic stiffening is accounted for. The tip mass has a 'softening' effect on the hub-beam system in TLAM, but has a 'stiffening' effect in FOAM. Theoretical analysis and simulation results show that FOAM has better adaptability than TLAM, especially in cases with high rotational speeds. The results above can be for reference when modeling and control of robot manipulators with payloads.

APPENDIX

The coefficients and matrices in the motion equation of the tip mass are given as follows:

$$\begin{aligned} M^l_{\theta\theta} &= m_t\left(r_A + l\right)^2 + m_t\boldsymbol{q}_1^T\phi_1^T(l)\phi_1(l)\boldsymbol{q}_1 \\ &\quad + m_t\boldsymbol{q}_2^T\phi_2^T(l)\phi_2(l)\boldsymbol{q}_2 + 2m_t\left(r_A + L\right)\phi_1(l)\boldsymbol{q}_1 \\ &\quad - m_t\left(r_A + L\right)\boldsymbol{q}_2^T\boldsymbol{S}\boldsymbol{q}_2 \end{aligned} \tag{A.1}$$

$$\boldsymbol{M}^l_{q_1\theta} = \left(\boldsymbol{M}^l_{\theta q_1}\right)^T = -m_t\phi_1^T(l)\phi_2(l)\boldsymbol{q}_2 \tag{A.2}$$

$$\boldsymbol{M}^l_{\theta q_2} = \left(\boldsymbol{M}^l_{q_2\theta}\right)^T = m_t\left(r_A + L\right)\phi_2(l) + \boldsymbol{q}_1^T m_t\phi_1^T(l)\phi_2(l) \tag{A.3}$$

$$\boldsymbol{M}^l_{q_1q_1} = m_t\phi_1^T(l)\phi_1(l) \tag{A.4}$$

$$\boldsymbol{M}^l_{q_2q_2} = m_t\phi_2^T(l)\phi_2(l) \tag{A.5}$$

$$\boldsymbol{G}^l_{q_1q_2} = -\left(\boldsymbol{G}^l_{q_2q_1}\right)^T = -m_t\phi_1^T(l)\phi_2(l) \tag{A.6}$$

$$\boldsymbol{K}^l_{q_1q_1} = -m_t\phi_1^T(l)\phi_1(l)\dot{\theta}^2 \tag{A.7}$$

$$\boldsymbol{K}^l_{q_2q_2} = -m_t\phi_2^T(l)\phi_2(l)\dot{\theta}^2 + m_t\left(r_A + L\right)\dot{\theta}^2\boldsymbol{S} \tag{A.8}$$

$$\begin{aligned} \boldsymbol{Q}^l_\theta = -\dot{\theta}\Big[& m_t\boldsymbol{q}_1^T\phi_1^T(l)\phi_1(l)\dot{\boldsymbol{q}}_1 + m_t\boldsymbol{q}_2^T\phi_2^T(l)\phi_2(l)\dot{\boldsymbol{q}}_2 \\ & + m_t\left(r_A + L\right)\phi_1(l)\dot{\boldsymbol{q}}_1 - m_t\left(r_A + L\right)\boldsymbol{q}_2^T\boldsymbol{S}\dot{\boldsymbol{q}}_2\Big] \end{aligned} \tag{A.9}$$

$$\boldsymbol{Q}^l_{q_1} = m_t\left(r_A + L\right)\dot{\theta}^2\phi_1^T(l) \tag{A.10}$$

REFERENCES

[1] T. R. Kane, R. R. Ryan, and A. K. Banerjee, "Dynamics of a cantilever beam attached to a moving base," *Journal of Guidance, Control, and Dynamics*, vol.10, no.2, pp. 139-150, 1987.

[2] R. Jeha, K. Sung-Sup, and K. Sung-Soo, "A general approach to stress stiffening effects on flexible multibody dynamic systems," *Mechanics of Structures and Machines*, vol.22, no.2, pp. 157-180, 1994.

[3] P. Shi, J. Mcphee, and G. R. Heppler, "A deformation field for Euler-Bernoulli beams with applications to flexible multibody dynamics," *Multibody System Dynamics*, no.5, pp. 79-104, 2001.

[4] A. K. Banerjee and J. M. Dickens, "Dynamics of an arbitrary flexible body in large rotation and translation," *Journal of Guidance, Control, and Dynamics*, vol.13, no.2, pp. 221-227, 1990.

[5] J. Mayo and J. Dominguez, "Geometrically nonlinear formulation of flexible multibody systems in terms of beam elements: geometric stiffness," *Computers and Structures*, vol.59, pp. 1039-1050, 1996.

[6] J. Hong and C. You, "Advances in dynamics of rigid-flexible coupling system," *Journal of Dynamics and Control*, vol.2, no.2, pp. 1-6, 2004. (in Chinese).

[7] H. Yang, J. Hong, and Z. Yu, "Dynamics modeling of a flexible hub-beam system with a tip mass," *Journal of Sound and Vibration*, vol.266, no.4, pp. 759-774, 2003.

[8] J. Liu and J. Hong, "Geometric stiffening of flexible link system with large overall motion," *Computers and Structures*, vol.81, pp. 2829-2841, 2003.

[9] J. Jang and D. Li, "Research on rigid-flexible coupling dynamics of spacecraft with solar panel " *Acta Aeronautica et Astronautica Sinica*, vol.27, no.3, pp. 418-422., 2006. (in Chinese).